ACS OMEGA

http://pubs.acs.org/journal/acsodf

Article

Cosmetic-Derived Mannosylerythritol Lipid-B-Phospholipid Nanoliposome: An Acid-Stabilized Carrier for Efficient Gastromucosal Delivery of Amoxicillin for In Vivo Treatment of *Helicobacter pylori*

Yanping Wu, Jiayue Geng, Xiaohong Cheng, Ying Yang, Yu Yu, Lili Wang, Quanjiang Dong, Zhe Chi, and Chenguang Liu*

Cite This: *ACS Omega* 2022, 7, 29086−29099

Read Online

ACCESS | Metrics & More | Article Recommendations | Supporting Information

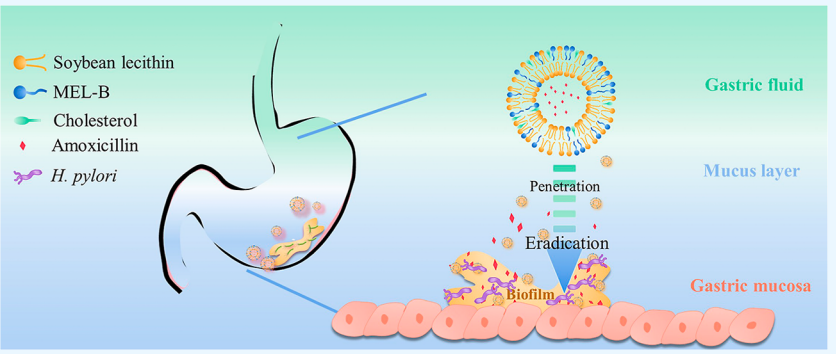

ABSTRACT: *Helicobacter pylori* infection is a leading cause of gastritis and peptic ulcer. Current treatments for *H. pylori* are limited by the increase in antibiotic-resistant strains and low drug delivery to the infection site, indicating the need for effective delivery systems of antibiotics. Although liposomes are the most successful drug delivery carriers that have already been applied commercially, their acidic stability still stands as a problem. Herein, we developed a novel nanoliposome using cosmetic raw materials of mannosylerythritol lipid-B (MEL-B), soy bean lecithin, and cholesterol, namely, LipoSC-MELB. LipoSC-MELB exhibited enhanced stability under the simulated gastric-acid condition, owing to its strong intermolecular hydrogen-bond interactions caused by the incorporation of MEL-B. Moreover, amoxicillin-loaded LipoSC-MELB (LipoSC-MELB/AMX) had a particle size of approximately 100 nm and exhibited sustained drug release under varying pH conditions (pH 3−7). Besides, LipoSC-MELB/AMX exhibited significantly higher anti-*H. pylori* and anti-*H. pylori* biofilm activity as compared with free AMX. Furthermore, LipoSC-MELB was able to carry AMX across the barriers of gastric mucus and *H. pylori* biofilms. Remarkably, in vivo assays indicated that LipoSC-MELB/AMX was effective in treating *H. pylori* infection and its associated gastritis and gastric ulcers. Overall, the findings of this study showed that LipoSC-MELB was effective for gastromucosal delivery of amoxicillin to improve its bioavailability for the treatment of *H. pylori* infection.

INTRODUCTION

Helicobacter pylori (*H. pylori*) is the leading cause of gastritis and peptic ulcer disease in humans,[1] with a prevalence rate of 50% in developed countries and 70−90% in developing countries.[2] Long-term *H. pylori* infection has been implicated in gastric cancers, such as gastric mucosa-associated lymphoid tissue lymphoma and adenocarcinomas. Moreover, it has been related to some other associated syndromes, such as idiopathic thrombocytopenic purpura, iron deficiency anemia, ischemic heart disease, stroke, Parkinson's disease, and Alzheimer's disease.[3] Thus, complete eradication of *H. pylori* is imperative to eliminate the human health risks of this bacterium. Currently, clarithromycin triple therapy or bismuth quadruple therapy is the first-line treatment against *H. pylori* infections.[4,5] However, these treatments are limited by their side effects and high doses that lead to gut dysbacteriosis.[3] Additionally, antibiotics, such as amoxicillin and clarithromycin, are easily degraded in gastric acid, and their absorption into the deeper layers of the gastric mucosa is barricaded by the gastric mucus layer.[3] Moreover, there has been an increase in antibiotic

Received: May 12, 2022
Accepted: August 3, 2022
Published: August 15, 2022

resistance strains of *H. pylori* due to indiscriminate antibiotic use and the presence of *H. pylori* biofilms.[6,7]

Over the years, studies have focused on overcoming the limitations of *H. pylori* therapies,[5] one of which is the development of drug delivery systems, such as nanocarriers. Nanocarriers can improve drug bioavailability by protecting encapsulated drugs from the adverse gastric environment and facilitating penetration of the mucosal barrier, so that to efficiently deliver drugs to target sites.[3,8] These nanocarriers include nanostructured lipid carriers, liposomes, nanoemulsions, metallic nanoparticles, polymeric nanoparticles, and microtechnological systems.[8] Among them, liposomes are promising nanoparticles for the treatment of *H. pylori* infection because of their biocompatibility, highly efficient encapsulation of both hydrophilic and hydrophobic drugs, and drug protection in the gastric environment.[8] Moreover, liposomes have already been commercialized for medical applications.[9] To date, many studies have evaluated the efficiency of liposomes as drug delivery carriers against *H. pylori*.[3,5,8] However, research findings have shown that most liposomes are thermodynamically and dynamically unstable because some of their components are vulnerable to environmental factors, such as ions, pH, and temperature.[10] Additionally, they are unsuitable for oral administration because they are unstable during storage and in the biological milieu.[11] Facing these challenges, efforts have been made to enhance the gastric acid resistance and stability of liposomes. Examples may include, but not exhaustive, the liposome-incorporated (2,3-dioleoyloxy-propyl)-trimethylammonium-chloride (DOTAP) and 1,2-dioleoyl-*sn*-glycero-3-phosphoethanolamine (DOPE) that are stable in simulated gastric juice;[12] the lecithin phospholipid bilayer-coated $CaCO_3$-cored nanoliposome to fast consume the excessive gastric acid;[13] and liposomes prepared with synthesized cholesteryl tetraethyleneglycol *N*-acetylglucosamine,[14] poly (acrylic acid)- and poly (allylamine hydrochloride)-coated liposomes,[11] lecithin and cholesterol coated with pectin, and L-α-phosphatidylcholine-mannosylerythritol lipid-A liposome,[15] for resisting the acidic environment in the gastric fluid. It appears that more easily available commodities shall be explored for fabricating such stabilized liposomes, paving the foundations for real translations of liposomes into the medical use to eradicate *H. pylori* infection.

MELs are a group of nonionic biosurfactants produced by fungi and yeasts, and they can be classified into four homologues, including MEL-A, MEL-B, MEL-C, and MEL-D, according to their degrees of acetylation.[16] Recently, MELs have received considerable research interest in the biomedical, pharmaceutical, and cosmetic fields because of their favorable characteristics, including biocompatibility, biodegradability, and environmental compatibility.[17] Importantly, MELs are reportedly stable under extreme pH and ionic strength conditions.[15] This advantage has instigated several in vitro studies to evaluate the stability and drug release profile of PC-MEL-A liposomes in acidic environments. Moreover, incorporation of MEL-A significantly increases the negative ζ potentials (from 50 to 75 mV to a negative value of −14.6 and −21.7 mV) and decreases the surface pH levels of the MEL-A-modified cholesteryl-3β-carboxyamindoethylene-*N*-hydroxyethylamine (OH-Chol) liposomes by affecting the protonation of the secondary amine in OH-Chol.[18] The findings of a previous study indicated that the molecular interaction via hydrogen bonds between MEL-A and liposome components may contribute to the enhanced stability against gastric acid.[15] Based on these findings, we hypothesized that MELs can be incorporated into liposomes to form an acid-resistant carrier for delivering antibiotics and effective treatment of *H. pylori* infection in vivo.

Therefore, the aim of this study was to examine the antibiotic delivery efficiency of MEL-B-liposome complexes for effective treatment of *H. pylori*. To achieve this, we used biosafe materials, including soybean lecithin (SL), cholesterol (Chol), and MEL-B, to prepare a drug delivery complex liposome (LipoSC-MELB). SL and Chol are common and low-cost chemicals, while cholesterol can significantly stabilize liposomes in vivo.[19] Moreover, MEL-B (Ceramela, TOYOBO) is the only commercially available mannosylerythritol lipid. Notably, the multiple hydroxyl groups in MEL-B may enable it to form stronger hydrogen-bond interactions within the liposome to resist harsh external environmental conditions. In this work, studies will be performed to justify the acid stability of LipoSC-MELB and contribution from the assumed hydrogen-bond interactions. Moreover, assays are carried out to investigate whether LipoSC-MELB can efficiently load amoxicillin, which is the most effective first-line anti-*H. pylori* drug and bears the lowest resistance by *H. pylori*.[20] Importantly, the amoxicillin-loaded LipoSC-MELB is assayed to specify its properties of drug release against different pH conditions, in vitro anti-*H. pylori* and anti-*H. pylori* biofilm efficacy, toxicity, capabilities of mucus retention and diffusion, and mucus and biofilm penetration that are able to contribute to the improved bioavailability of amoxicillin. At last, the in vivo therapeutic effect for *H. pylori* of amoxicillin-loaded LipoSC-MELB will be conducted to validate whether this liposome has an enhanced efficacy. These are presented in detail in this work, hoping to offer a novel liposome with enhanced acid stability for gastromucosal delivery of amoxicillin to eradicate *H. pylori* infection.

MATERIALS AND METHODS

Reagents, Cells, Strains, and Cultivation. Mannosylerythritol lipid-B [MEL-B, hydrophile−lipophile balance (HLB) value ∼9] from Toyobo Co., Ltd. (Osaka, Japan), namely, "Ceramela", was kindly provided by Qingdao Youdo Bioengineering Co., Ltd. (Qingdao, China). Sucrose fatty stearic acid ester S-1170 (HLB ∼ 11) was purchased from Mitsubishi Chemical Corp. (Tokyo, Japan), Tween 80 (HLB ∼ 15) was procured from Sigma-Aldrich LLC. (St. Louis, MO, USA), and Alexa Fluor 594 cadaverine dye was purchased from Thermo Fisher Scientific Inc. (Waltham, MA, USA). Fluorescein sodium (FLNa) was purchased from Sigma-Aldrich LLC. (St. Louis, MO, USA). Soy lecithin, cholesterol, amoxicillin (AMX), 3-(4, 5-dimethyl-2-thiazolyl)-2, 5-diphenyl-2-H-tetrazolium bromide (MTT), chloroform, and 1 × PBS buffer (pH 7.4) were purchased from Shanghai Yuanye Bio-Technology Co., Ltd. (Shanghai, China). F12K complete medium was purchased from Thermo Fisher Scientific Inc. (Waltham, MA, USA). All regular reagents used were of analytical grade. The human gastric carcinoma AGS cell line was purchased from the American Type Culture Collection (CRL-1739). *H. pylori* Sydney Strain 1 (SS1) was provided by the Central Laboratory and Department of Gastroenterology, Qingdao Municipal Hospital. *H. pylori* SS1 strain was cultivated for 72 h on Karmali agar medium (Oxoid, UK) or in Karmali liquid medium supplemented with defibrinated sheep blood (5%, v/v) (Sinova-HK Biotechnology Co., Ltd., Qingdao, China) and *H. pylori* selective supplement (Dent)

https://doi.org/10.1021/acsomega.2c02953
ACS Omega 2022, 7, 29086−29099

(Oxoid, UK), at the concentration instructed by the manufacturer under microaerophilic conditions at 37.0 °C. Bacterial concentration was determined by measuring the optical density at 600 nm using a UV−vis spectrophotometer (PERSEE, Beijing, China).

Preparation and Characterization of Liposomes. Liposomes were prepared using thin-film hydration methods with ultrasonication.[21] For the SL and cholesterol liposomes, 10.0 mg of SL and 2.0 mg of cholesterol were dissolved in 2.0 mL of chloroform in a round bottom flask. Then, the chloroform was evaporated in a water bath at 70.0 °C placed in a fume hood for 5 min to form thin lipid films. The lipid films were resuspended in pure water by magnetic stirring for 30 min, and the resulting lipid suspension was processed by ultrasonication (Scientz, Ningbo, China) (40.0% kW, working: 2 s, interval: 2 s, cycle duration: 10.0 min) in an ice bath to obtain liposomes. For the surfactant-modified liposomes, 10.0 mg of SL, 2.0 mg of cholesterol, and different amounts of surfactants according to the weight ratio were used as the precursors for the liposome, using the abovementioned procedures. For amoxicillin (AMX)-loaded liposomes, 10.0 mg of thin lipid films was resuspended in 10.0 mL of solution containing 0.1 mg/mL AMX to obtain AMX-loaded liposomes. Liposome formation was also achieved by ultrasonication under the conditions described above. The particle size, polydispersity index (PDI), and ζ potential of each sample were measured using a Zetasizer Nano-S90 instrument (Malvern, UK). Structural groups and interactions between the components of the liposomes were analyzed using a Fourier transform infrared (FT-IR) spectrometer (Thermo Fisher Scientific, USA).

The encapsulation efficiency (EE) and drug loading capacity (DL) of amoxicillin by liposomes were determined as previously described.[2] Briefly, 1 mL of AMX-loaded liposomes (1 mg/mL) was placed in a 10.0 kDa Millipore ultrafiltration tube (Millipore, USA), followed by centrifugation at 10,000 *g* for 10 min. The amount of free AMX in the eluent was determined using HPLC.[22] EE was calculated using the following equation

$$\text{EE}\ (\%) = \frac{\text{total amount of AMX} - \text{free amount of AMX}}{\text{total amount of AMX}} \times 100\%$$

$$\text{DL}\ (\%) = \frac{\text{total amount of AMX} - \text{free amount of AMX}}{\text{total amount of liposome}} \times 100\%$$

In Vitro pH Stability and Drug Release. The in vitro pH stability of liposomes was determined by placing them in 20 mM PBS buffer of different pH (3.0−7.0) values at 25 °C for 12 h. The particle sizes of the treated liposomes were measured using Zetasizer Nano S90 (Malvern, UK). Evaluation of in vitro drug release was performed using the dialysis diffusion method for 2.0 mL of 1 mg/mL liposome suspension (encapsulating 0.1 mg/mL AMX) in a dialysis bag (MWCO = 3.5−5 kD) under conditions previously specified,[21,23] and the concentration of AMX was determined by HPLC.[22] Particularly, phase-dependent drug release was evaluated. In detail, a 9 h drug release test was performed for the AMX-loaded liposomes. During the first 2 h, drug release from the AMX-loaded liposome was examined in the simulated gastric fluid environment (pH 3.0).[24] Thereafter, the AMX-loaded liposome was transferred into a mucin-containing (30 μg/mL)[25] PBS solution (pH 4.5) to simulate the gastric luminal mucus layer,[23,26] and drug release was recorded for another 2 h. At last, the AMX-loaded liposomes were transferred into mucin-containing PBS solution (pH 6.6) to simulate the gastric adherent mucus layer, and drug release was examined for another 5 h. At specific time points, 1 mL of dialysate aliquots was collected (the deficit was replenished with fresh solution of equivalent volume), filtered through a 0.22 μm polycarbonate filter membrane, and the AMX content was measured by HPLC.[22]

Anti-*H. pylori* and Anti-*H. pylori* Biofilm Activity. The anti-*H. pylori* SS1 and anti-*H. pylori* SS1 biofilm activities of AMX-loaded liposomes were evaluated in vitro. Where needed, the treatment to the planktonic *H. pylori* SS1 or *H. pylori* SS1 biofilm with free AMX as the positive control group, with the empty MEL-B modified liposomes as the blank group, and with 1 × PBS buffer (pH 7.4) as the negative control group was carried out. The concentration of AMX was 5 μg/mL, and the concentrations of AMX-loaded and empty liposomes were both 1 mg/mL.

The anti-*H. pylori* SS1 activity was determined using freshly cultivated planktonic *H. pylori* SS1 cells following a previously described method[27] with some modifications. Briefly, *H. pylori* SS1 strain was cultured on Karmali agar medium in a microaerobic environment (10% CO_2, 85% N_2, and 5% O_2) at 37 °C for 2−3 days; then, the fresh colonies on the agar plate were harvested into liquid Karmali medium containing 10% (v/v) fetal bovine serum and 0.2% (w/v) Dent, and the final cell density was adjusted to the optical density at 600 nm (OD_{600nm}) of 0.1. The bacterial suspension (150 μL) was then inoculated into 96-well plates, and 50 μL of different purposed solutions was subjected to the bacterial cells in the well. The 96-well plates were then cultured in the microaerobic environment at 37 °C with shaking (100 rpm), and the absorbance at 600 nm was measured after 24 h. Bacterial viability (%) = (Is − Ib)/(Ic − Ib) × 100%, where Ic, Ib, and Is represented the average OD of the control groups (bacteria without any treatment), blank groups (without bacteria), and the experimental groups (bacteria treated with different solutions), respectively.

Additionally, the ability of AMX-loaded liposomes to eradicate the mature biofilms of *H. pylori* SS1 was evaluated by crystal violet (CV) staining.[28] Briefly, the *H. pylori* SS1 biofilm was cultured in sterile 96-well plates as described above.[28] After cultivating for 72 h, the medium was replaced with different purposed solutions. The plates were incubated in the microaerobic environment at 37 °C for another 24 h. Then, the supernatant was removed, and PBS was added to rinse the biofilm to remove the planktonic cells. After drying at 37 °C, the biofilm was stained with 0.5% crystal violet solution for 15 min. Finally, 200 μL of ethanol (95%) was added to determine the biofilm biomass by measuring the absorbance of the ethanol solution at 570 nm.

Gastric Retention, Mucus, and Biofilm Penetration Assays. The gastric retention of AMX-loaded liposomes was evaluated by referring to the method described previously.[29] Alexa Fluor 594 cadaverine dye (FL594) was used to label the liposomes for this assay. The FL594-labeled AMX-loaded liposome was prepared according to the abovementioned procedures, with the aqueous phase containing 0.01 mM FL594 and 0.1 mg/mL AMX. The free FL594 and AMX were removed by ultrafiltration centrifugation (MWCO = 3 kD,

https://doi.org/10.1021/acsomega.2c02953
ACS Omega 2022, 7, 29086−29099

(a)

Formula (w/w)	Size (nm)	PDI	Zeta potential (mV)
SL/Chol (5:1)	116.9 ± 0.5[a]	0.22 ± 0.01[b]	-30.5
SL/Chol/MEL-B (5:1:1)	106.9 ± 0.5[b]	0.27 ± 0.01[b]	-34.3
SL/Chol/MEL-B (5:1:2)	107.7 ± 0.7[b]	0.26 ± 0.02[b]	-34.4
SL/Chol/MEL-B (5:1:3)	104.3 ± 0.2[c]	0.25 ± 0.01[b]	-35.4
SL/Chol/MEL-B (5:1:4)	79.5 ± 0.1[e]	0.36 ± 0.01[a]	-40.2
SL/Chol/TW80	63.4 ± 0.1[f]	0.34 ± 0.01[a]	-6.93
SL/Chol/SE-S1170	102.5 ± 0.1[d]	0.22 ± 0.02[b]	-24.01

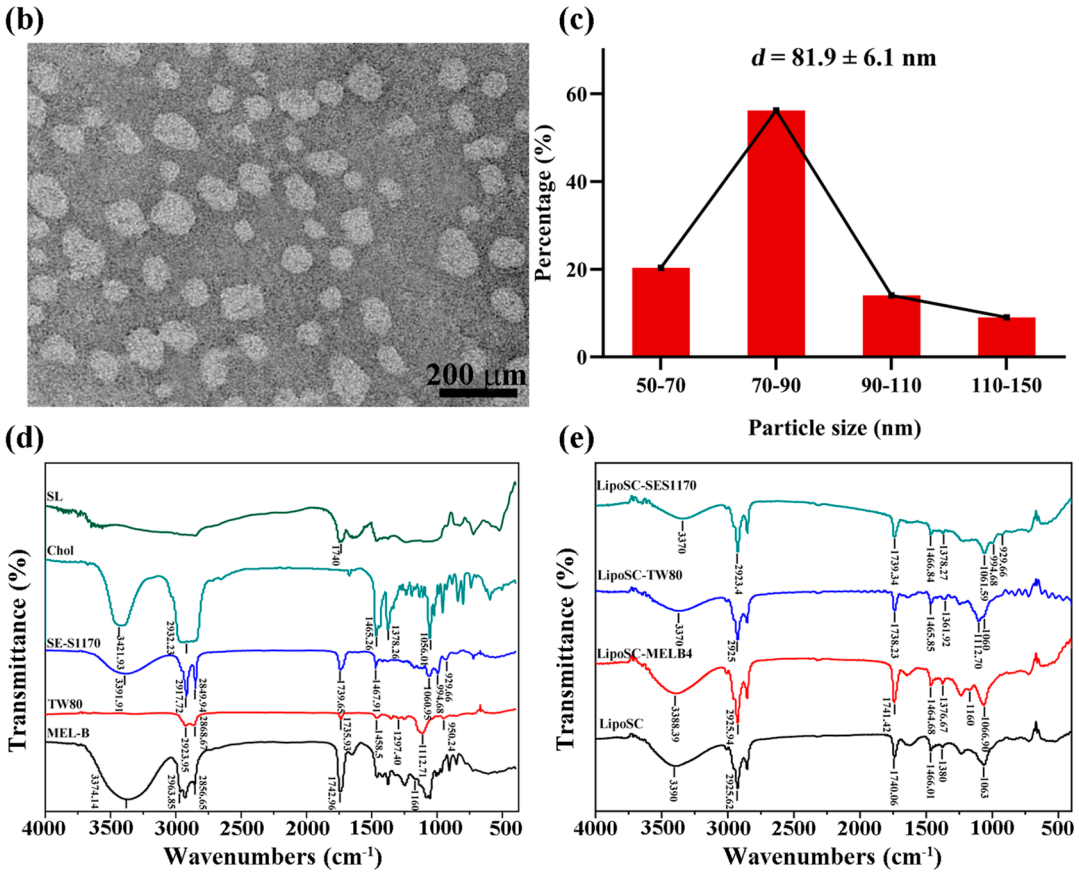

Figure 1. Characterization of liposomes generated in this study. (a) Formulation of liposomes with different average particle sizes, PDIs, and ζ potentials. (b) TEM observation of LipoSC-MELB liposomes obtained using SL, cholesterol, and mannosylerythritol lipid-B at 5:1:4 (LipoSC-MELB4). (c) Average particle size and size distribution of LipoSC-MELB4 measured by TEM. (d,e) FT-IR analysis for the liposome precursors and the prepared liposomes. Data, where necessary, are presented as means ± SD (n = 3). Data with different superscript letters in the same column are significantly different ($p < 0.05$).

5000g, 10 min).[31] In vivo imaging was performed using an in vivo imaging apparatus (Newton 7.0, Vilber, USA). Laser confocal microscopy was performed using an LSM 800 laser confocal microscope (Carl Zeiss, Oberkochen, Germany).

In vitro gastric mucus penetration of AMX-loaded liposomes was assayed using a Transwell system.[30] FLNa was used as the fluorescent probe to quantify mucus penetration of the liposomes, and the FLNA-labeled AMX-loaded liposomes were also prepared as described above. Gastric mucus was scraped from fresh pig stomachs and stored at −80 °C until use. Before the experiment, the frozen mucus was thawed in an incubator at 37 °C.[31] To perform the assay, 50 μL of gastric mucus was added to a Transwell insert (12-well plate, Corning, USA) with a polycarbonate film (3.0 μm pore size). Next, 100 μL of 1 mg/mL FLNa-labeled-AMX-loaded liposomes (containing 0.1 mg/mL AMX and 0.01 mM FLNa) was added onto the mucus surface, and the plate was incubated in a shaker at 37 °C (100 rpm). The remaining operations strictly followed the procedures in the previous work.[30] Liposome penetration was tracked using a laser confocal microscope (ZEISS LSM 800, Carl Zeiss, USA) in the Z-stacking scanning mode.[31] DAPI was added to the mucus for fluorescence contrast. The aggregation rate and apparent permeability coefficient (Papp) were calculated as described previously.[30]

https://doi.org/10.1021/acsomega.2c02953
ACS Omega 2022, 7, 29086−29099

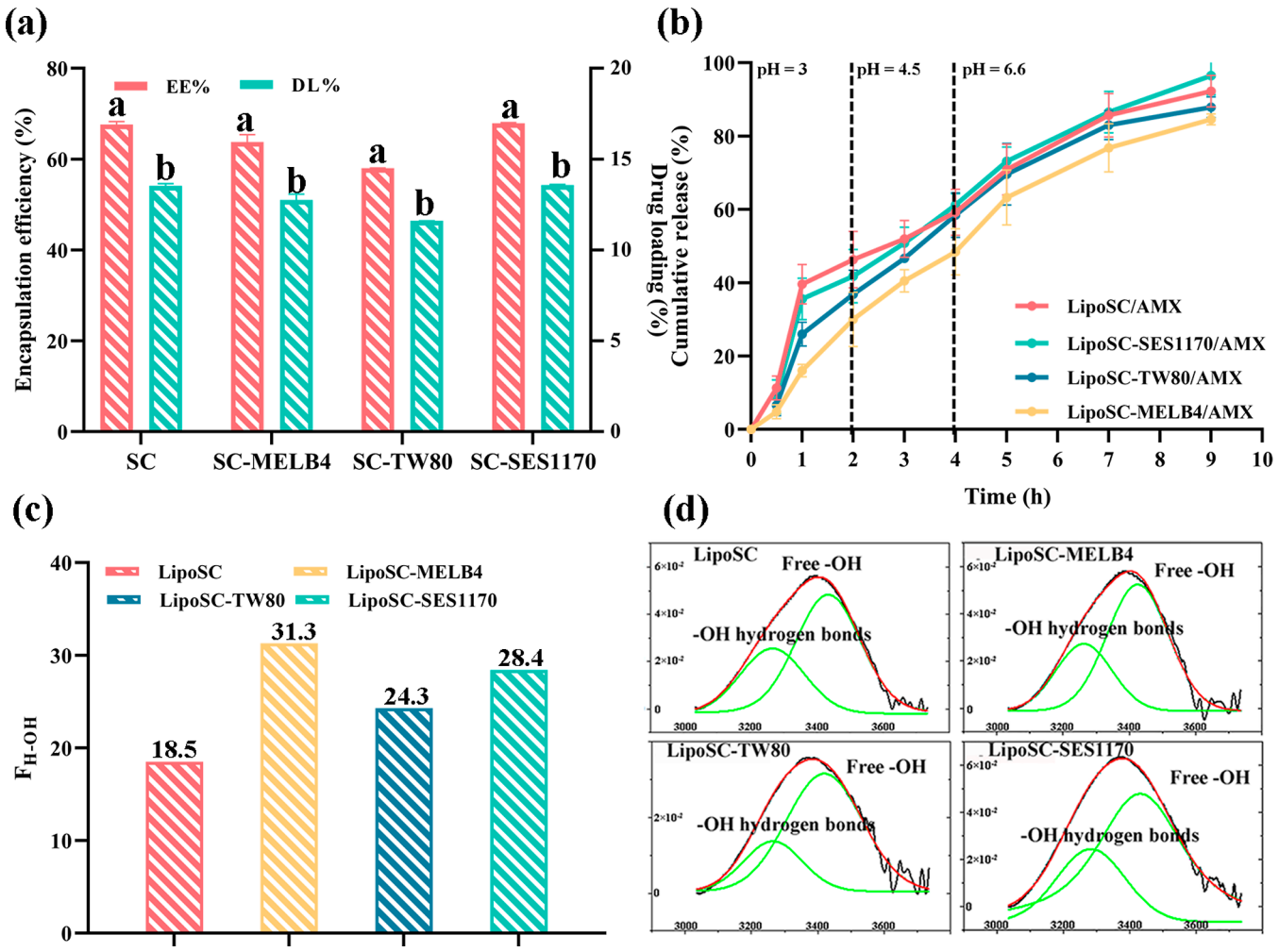

Figure 2. (a) Encapsulation efficiencies and amoxicillin loading in the liposomes, including LipoSC (SC), LipoSC-MELB4 (MELB4), LipoSC-TW80 (TW80), and LipoSC-SES1170 (SE-S1170). Data with different letters are significantly different ($P < 0.05$). (b) Amoxicillin release profiles from liposomes under varying pH conditions. (c) Hydrogen-bonding fraction values of the specific liposomes. (d) High-resolution FT-IR spectra displaying the fractions of free and hydrogen-bond-forming hydroxyl groups for specific liposomes. Data, where necessary, are presented as means ± SD ($n = 3$).

To evaluate the in vitro biofilm penetration of the MEL-B-modified liposomes, they were labeled with Nile red. *H. pylori* SS1 biofilms were cultured on sterile 24-well plates and then stained for 1 h with DAPI (5.0 μg/mL) for fluorescence contrast. Then, 100 μL of liposomes containing Nile red (5.0 μg/mL) was gently added to the biofilm surface. The biofilm penetration of liposomes was recorded using a laser confocal microscope (ZEISS LSM 800, Carl Zeiss, USA) in the Z-stacking scanning mode.[32]

Toxicity Evaluation. The cytotoxicity of the liposomes in this work was evaluated by performing MTT assay using human gastric carcinoma AGS cells.[23] The cells were cultured in F12K complete medium at 37 °C in a 5% CO_2 atmosphere. AGS cells (1.0×10^5) were seeded into 96-well plates and cultured for 24 h. Then, AGS cells were incubated with the liposome suspensions in different concentrations for 24 h. Afterward, the liposome solution was replaced with sterile MTT solution (100 μL, 0.5 mg/mL) and incubated for 4 h. After removing the MTT, 100 μL of DMSO was added into each well, and OD values were measured at 570 nm. Cell viability rate was expressed as the relative percentage compared to the untreated group.

The acute toxicity of liposomes was assessed using healthy C57BL/6 mice (male, 6−8 week old, 20−22 g).[33] Mice were divided into different groups ($n = 6$), and each group was administered liposomes at the intended dose three times a day via oral gavage for 1 day. The mice were observed for 7 days after administration, and toxicity was assessed by observing mortality, weight loss, and appearance.[34]

In Vivo Assay. Animal assays were approved and supervised by the Animal Ethics Committee of the Ocean University of China and Qingdao Municipal Hospital. All animal assays were conducted by trained personnel, and animal suffering was minimized. After the animal assay was completed, the animals were anesthetized and sacrificed. The corpses were disposed of by a specific agency at Qingdao Municipal Hospital. An animal model with simultaneous *H. pylori* SS1 infection and gastric ulcers was established in C57BL/six mice (male, 6−8 week old, 20−22 g) following previously described procedures.[35] *H. pylori*-infected mice were randomly divided into three groups ($n = 6$) and administered AMX (14.0 mg/kg), LipoSC-MELB/AMX (dosage weighed in amoxicillin at 14 mg/kg), or an equal volume of PBS buffer once a day for 7 days. The mice were sacrificed 48 h after the last

https://doi.org/10.1021/acsomega.2c02953
ACS Omega 2022, 7, 29086−29099

administration, and the gastric segment was located after laparotomy. The gastric contents were removed and washed with 0.9% sterile NaCl solution. The gastric tissues were divided into two parts: one was subjected to paraformaldehyde fixation and paraffin embedding, while the other was used for *H. pylori* quantitative culture[36] by spreading the minced tissues on Karmali agar medium supplemented with defibrinated sheep blood (5%, v/v) and Dent (0.2%, w/v).

The embedded gastric tissues were processed by performing H & E and Giemsa staining.[36,37] Immunohistochemical analysis was performed to evaluate the levels of the proinflammatory factors IL-1β and TNF-α in mouse serum using ELISA kits. Fluorescence staining for Occludin-1 and ZO-1 proteins was performed to assess the integrity of the gastric mucosa in fresh gastric tissue.[38]

Statistical Analysis. Statistical analysis was performed using GraphPad Prism 5 (GraphPad Software Inc., USA). Experiments were conducted in triplicate (n = 3) or sextuplicate (n = 6) when necessary, and the results are expressed as the mean ± standard deviation. Comparative studies of means were performed using one-way analysis of variance, and statistical significance was set at $p < 0.05$.

RESULTS AND DISCUSSION

Formular Optimization and Characterization of Surfactant-Modified Liposomes. SL, cholesterol (Chol), and mannosylerythritol lipid-B (MEL-B) were used to prepare complex liposomes (LipoSC-MELB). Additionally, sucrose fatty stearic acid ester S-1170 and Tween-80 were used as surfactants alternative to MEL-B to prepare liposomes (LipoSC-SES1170 and LipoSC-TW80, respectively). First, SL-Chol liposomes (LipoSC) were prepared as scaffolds. The weight ratio of SL to cholesterol was optimized according to the average particle size and PDI.

As shown in Table S1, when the weight ratio of SL to Chol was 5:1, a minimal average particle size of 116.5 nm and a suitable PDI of 0.22 were obtained, indicating that this ratio was optimal for fabricating the liposome. Based on this, MEL-B was incorporated into the liposomes, and the particle size decreased with increasing amount of MEL-B (Figure 1a). Overall, at an SL/Chol/MEL-B of 5:1:4, the particle size of the resulting liposome (designated as LipoSC-MELB4) was smaller than 100 nm (79.5 ± 0.1 nm). Similarly, TEM observation confirmed that LipoSC-MELB4 was well-dispersed in the solution without aggregation (Figure 1b), with an average particle size of approximately 81.0 nm (Figure 1c). Compared with previous studies, the particle size of the gastric-stabilized liposome developed in the present study was smaller.[11,15,25] Previously, it was confirmed that the nanoparticle size accounted for the limitation of diffusion in the dense gastric mucus.[12] Thus, the smaller size of LipoSC-MELB4 implies its enhanced permeability in gastric mucus.

Furthermore, although the liposomes generated by incorporating SE-S1170 or Tween 80 with SL-Chol (SL/Chol/surfactant = 5:1:4) had similar particle size and PDI to those obtained using MEL-B, their ζ potentials (−24.0 and −6.9 mV, respectively) revealed that they possessed lower negative charge (Figure 1a). It was claimed that a ζ potential greater than 30 mV is sufficient to maintain electrostatically stabilized suspensions.[25] Therefore, considering the particle size and surface charge, LipoSC-MELB4 was the most suitable liposome.

The structural groups and interactions between the liposomal components were analyzed using FT-IR analysis. As shown in Figure 1d, the characteristic signals of Chol at 3421.93 cm^{-1} were due to unreacted −OH; the peak at 2932.23 cm^{-1} was due to unreacted C−H, the peak at 1465.26 cm^{-1} was due to C−H asymmetrical deformation vibration, and the peak at 1056.01 cm^{-1} was due to free C−O−H; the characteristic signals of SL at 1740.0 cm^{-1} were due to unreacted C═O (Figure 2e).[39,40] These data suggest that no covalent bonds were formed between Chol and SL during liposome formation. Moreover, the characteristic peak of −OH at 3421.93 cm^{-1} in Chol shifted to 3390 cm^{-1} in LipoSC, indicating the formation of hydrogen bonds between Chol and SL when the liposome was formed. Furthermore, the absorbance peak observed in Chol at 2932.23 cm^{-1} (Figure 1d), which was ascribed to the stretching vibrations of the CH_3 and CH_2 groups, decreased in LipoSC to 2925.62 cm^{-1} (Figure 1e). Except it, no other shift in the absorbance was observed. In the FT-IR spectra of liposomes modified with different surfactants (Figure 1e), the characteristic bands for LipoSC were consistently detected. Additionally, the characteristic bands of these surfactants were observed in the spectra of the surfactant-modified liposomes (Figure 1d). Specifically, the C−OH peak band at 1160.0 cm^{-1} in MEL-B was observed in the LipoSC-MELB spectrum, the C−O peak at 994.68 cm^{-1} and the D-glucopyranose peak at 929.66 cm^{-1} in SE-S1170 were observed in the LipoSC-S1170 spectrum,[41] and the C−O−C peak at 1100.50 cm^{-1} in Tween 80 was observed in the LipoSC-TW80 spectrum.[42] Notably, peak shift that occurred in the hydroxyl group region was commonly observed in the spectra compared with that of LipoSC, indicating that more hydrogen bonds were formed in the three surfactant-modified liposomes. More than this, no new vibrations were observed, thereby demonstrating successful physical incorporation of these surfactants into the resulting liposomes without forming new covalent bonds.

Gastric Stability, Drug Encapsulation, and Release of SC-MELB Liposomes. A critical feature of liposomes for gastric drug administration is its stability when exposed to the acidic environment in the stomach,[43] since this is important for effective delivery and protection of encapsulated drugs, as previously stated. To evaluate this property of LipoSC-MELB liposomes, LipoSC-MELB4 was subjected to different pH conditions (3.0−7.0) lasting 12 h, and the particle size and PDI were measured. Generally, there was no significant change in the average diameter of LipoSC-MELB4 under pH 4.0−7.0; however, there was a 20.5% increase (from approximately 77.5 to 93.4 nm) in the particle size at pH 3.0 (Figure S1a). Similar results were observed for LipoSC-SES1170 and LipoSC-TW80 (Figure S1b,c); however, the mean diameter of LipoSC increased considerably from 111.2 nm to approximately 169.6 nm (Figure S1d). These data indicated that the incorporation of surfactants reinforced the acid stability of the resulting liposomes. Generally, protonation of susceptible groups occurs under acidic conditions, resulting in an increase in proton concentration and conformational transformation of lipids, which can negatively affect the lipid bilayer structure of liposomes.[44] However, the incorporation of surfactants can also enhance intermolecular hydrogen bonding inside the liposomes, as revealed by FT-IR analysis (Figure 1e), thus increasing the stability and reducing the fluidity of the surfactant-modified liposomes in gastric acid.[15]

https://doi.org/10.1021/acsomega.2c02953
ACS Omega 2022, 7, 29086−29099

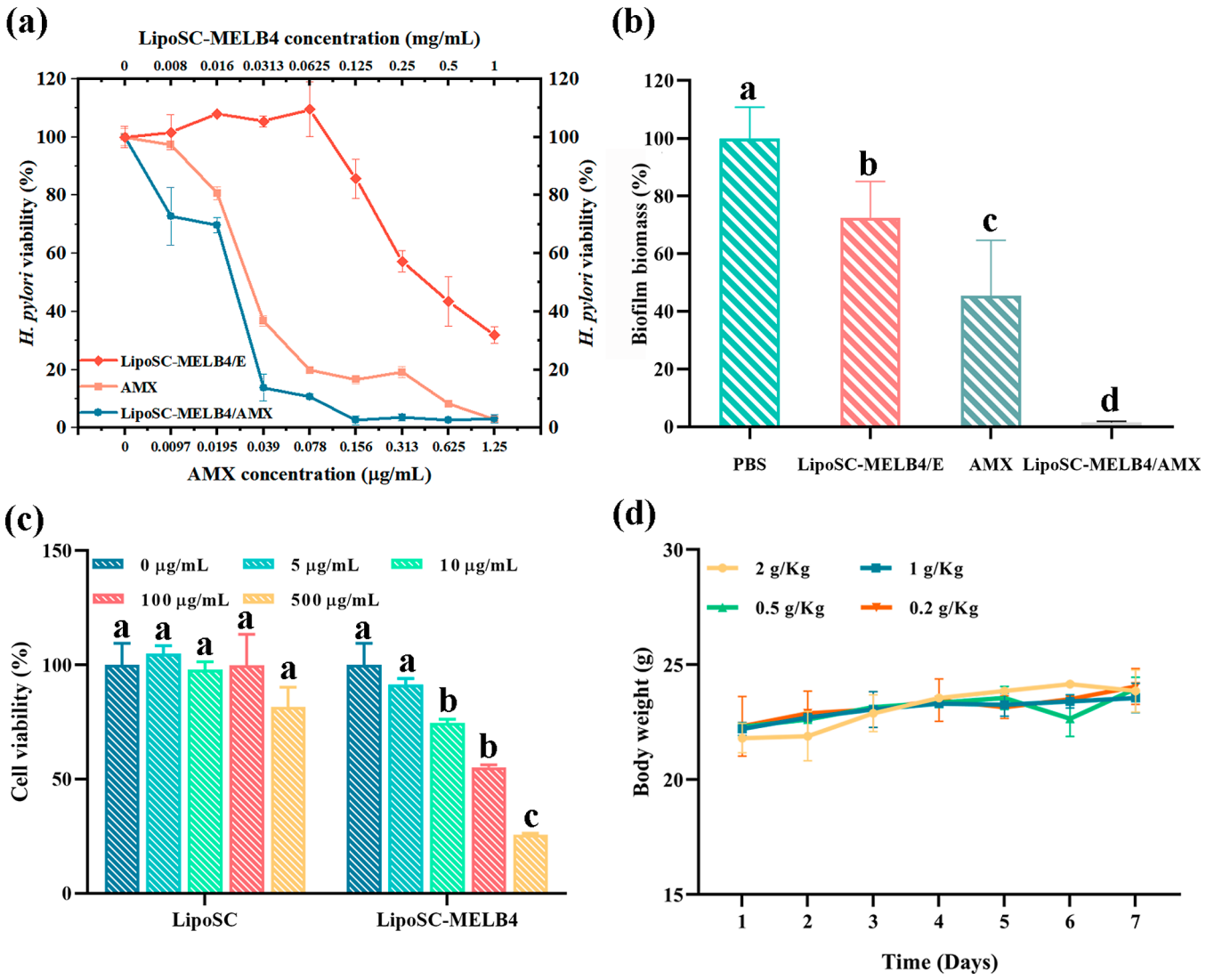

Figure 3. (a) Antibacterial activities of empty LipoSC-MELB4 (LipoSC-MELB4/E), free amoxicillin (AMX), and amoxicillin-loaded LipoSC-MELB4 (LipoSC-MELB4/AMX) against planktonic *H. pylori*. (b) Antibiofilm activities of 1 × PBS buffer as a negative control, LipoSC-MELB4/E, AMX, and LipoSC-MELB4/AMX against mature biofilms of *H. pylori*. (c) In vitro toxicity of LipoSC and LipoSC-MELB4 to human AGS cells. (d) In vivo acute toxicity of LipoSC-MELB4 in C57BL/6 mice. Data are presented as means ± SD (n = 3). Data with different letters in the same subfigure are statistically significant ($P < 0.05$).

The stability of LipoSC-MELB4 in the acidic environment indicated that it might be able to retain drugs within the encapsulation. To verify this, amoxicillin was encapsulated in LipoSC-MELB4, obtaining LipoSC-MELB4/AMX (particle size slightly increased to approximately 83.4 nm). The EE and DL of LipoSC-MELB4/AMX were determined; LipoSC, LipoSC-MELB4, and LipoSC-SES1170 had similar EE and DL (approximately 65.0 and 13.0%, respectively), whereas those for LipoSC-TW80 were slightly lower without a significant difference (Figure 2a and Table S2). To be noted, the EE of AMX by LipoSC-MELB4 (65.0%) was moderate, which was higher than that of the poly (allylamine hydrochloride)-coated liposome (47.7%),[11] similar to that of the uncoated lecithin/cholesterol liposome (66.0%),[25] and lower than that of the pectin-coated lecithin/cholesterol liposome (83.0%).[25] However, the DL capacity for AMX of LipoSC-MELB4 (13.0%) was higher than that for cetyl palmitate-based liposomes of less than 8.0%.[23]

Furthermore, the release of amoxicillin from these liposomes under varying pH conditions was profiled. As shown in Figure 2b, LipoSC-MELB4/AMX consistently displayed sustained release of amoxicillin under different pH values simulating the gastric lumen (pH 3.0),[24] luminal mucus layer (pH 4.5),[45] and adherent mucus layer (pH 6.6).[46] The final accumulative drug release rate was approximately 84.6% after 9 h. In contrast, although the other liposomes had higher cumulative release of amoxicillin after 9 h, they exhibited burst drug release in the first 1 h when exposed to simulated gastric fluid (approximately 26.0−40.0%) conditions compared with LipoSC-MELB4 (approximately 18.0%). Previous studies have reported similar sustained drug release for mannosylerythritol lipid-A-incorporated[15] and poly (acrylic acid)-coated[11] liposomes in a gastric acid-simulating environment. However, this is the first study to report sustained release of amoxicillin under conditions of pH values representing acidic to nearly neutral conditions.

https://doi.org/10.1021/acsomega.2c02953
ACS Omega 2022, 7, 29086−29099

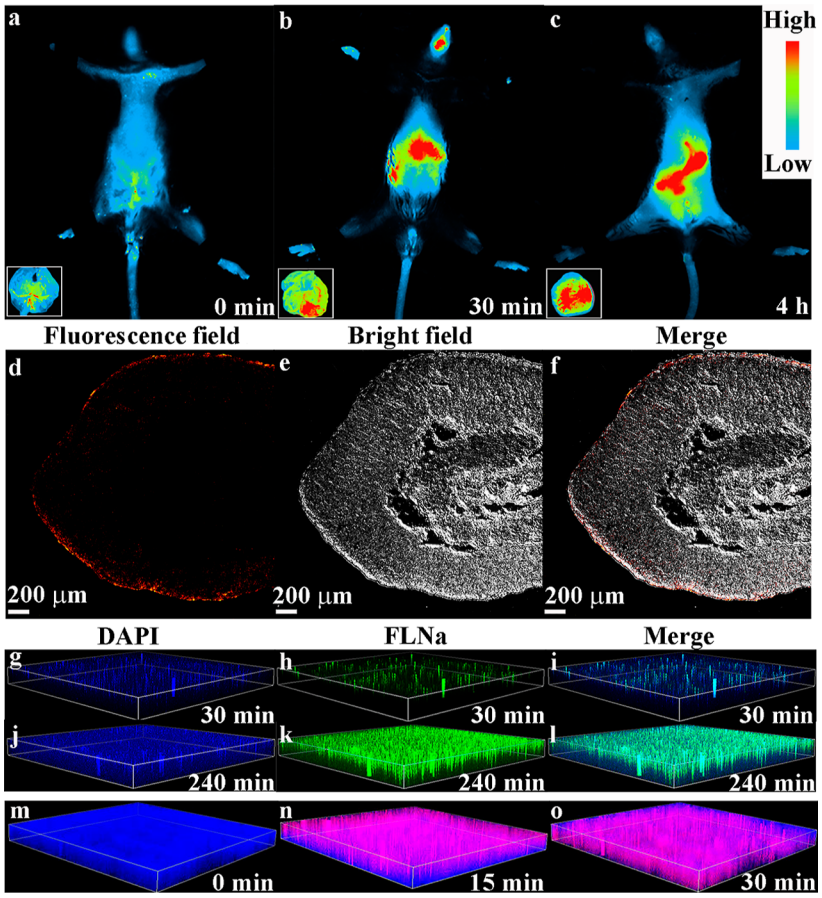

Figure 4. Retention, distribution, and mucus and biofilm penetration of LipoSC-MELB4. (a–c) In vivo imaging of gastric retention of Alexa Fluor 594 and amoxicillin coencapsulated LipoSC-MELB4 4 h after oral administration; excitation wavelength (λex) = 590 nm; emission wavelength (λem) = 617 nm; and color bar: fluorescence intensity. (d–f) Fluorescence- and bright-field confocal laser microscopy images of the transverse cryosections of mouse stomach tissues 4 h after intragastrical administration of LipoSC-MELB4/AMX-FL594; λex = 590.0 nm and λem = 617.0 nm. (g–l) Laser confocal microscopy images of fluorescent tracing of mucus penetration by fluorescein sodium and amoxicillin coencapsulated liposome LipoSC-MELB4 30 min and 240 min after oral gavage; λex = 491.0 nm and λem = 512.0 nm. (m–o) Laser confocal microscopy images of biofilm penetration for Neil red-encapsulated LipoSC-MELB4 at different time points; λex = 530.0 nm and λem = 635.0 nm.

The sustained drug release from LipoSC-MELB4/AMX in this study suggests a stronger hydrogen-bond interaction in LipoSC-MELB4. To validate this, high-resolution hydroxyl spectra from 3100 to 3600 cm^{-1} were curve-fitted. The bands located at approximately 3420 cm^{-1} were ascribed to the free −OH groups of Chol, and those near 3300 cm^{-1} were ascribed to OH in hydrogen bonds (Figure 2c).[47] Further determination of the hydrogen-bonding fraction (F_{H-OH}) according to these high-resolution spectra (Figure 2d) showed that the value for LipoSC-MELB (0.32) was the largest among those tested liposomes, confirming that the strongest intermolecular hydrogen-bond interaction[48,49] occurred in LipoSC-MELB. This could be attributed to the higher hydrophobicity of MEL-B than Tween 80 and SE-S1170, as indicated by the smaller HLB value of MEL-B, which might facilitate a stronger hydrophobic interaction between MEL-B and the other liposome components. This may be beneficial for the formation of intramolecular hydrogen bonds between the liposome components. Moreover, it could be inferred that the incorporation of a nonionic surfactant such as MEL-B, which contains multiple intramolecular short-chain acryl groups, into liposomes would lead to the formation of strong hydrogen bonds. This can be due to the higher polarity of this glycolipid, which causes its asymmetric distribution in the liposome layers, allowing the partitioning of MEL-B to strengthen the hydrogen-bond interaction.[15] Moreover, the shorter acryl group chains of MEL-B than those of Tween 80 and SE-S1170 indicate that MEL-B has a larger mass fraction of hydroxyl groups, which may render it to form more hydrogen bonds in LipoSC-MELB. However, this would require further study for validation.

Overall, these results indicated that LipoSC-MELB4 was the most suitable liposome in this work, as an acid-resistant carrier for gastric delivery of amoxicillin.

Anti-*H. pylori* Activity In Vitro and Toxicity of SC-MELB Liposomes. Following the verification of LipoSC-MELB4 as the most suitable liposome, the bactericidal activity of LipoSC-MELB4/AMX was evaluated in vitro. First, we evaluated the antibacterial activity of LipoSC-MELB4/AMX against planktonic *H. pylori*. Compared with free AMX (minimal bactericidal concentration of 0.625 μg/mL to kill 90.0% bacteria), LipoSC-MELB4/AMX exhibited improved antibacterial activity (Figure 3a), with a minimal bactericidal concentration (to kill 90.0% of bacteria)[27] of 0.078 μg/mL. In addition, it was found that the antibacterial effect on planktonic *H. pylori* from empty LipoSC-MELB4 only began to show at concentrations over 0.0625 mg/mL. The antibacterial effect of empty LipoSC-MELB4 was speculated

https://doi.org/10.1021/acsomega.2c02953
ACS Omega 2022, 7, 29086−29099

to be induced by liposome−bacterial membrane fusion as proposed previously.[50] However, this concentration was approximately 800 times greater than that of LipoSC-MELB4/AMX. Thus, at the same concentrations as low as those of LipoSC-MELB4/AMX, the antibacterial contribution from empty LipoSC-MELB4 was negligible.

Importantly, LipoSC-MELB4/AMX loading 5.0 μg/mL amoxicillin efficiently eradicated approximately 98.5% mature biofilms of *H. pylori* compared with free amoxicillin, which eradicated only 54.7% mature biofilms at the same concentration (Figure 3b). Moreover, the empty LipoSC-MELB4 could also exhibit an anti-*H. pylori* activity, but the clearance efficiency was too low (about 25.0%) to be effective. These results indicated from in vitro that the bioavailability of amoxicillin can be improved by the encapsulation into LipoSC-MELB4, most probably because of its nanosize and biofilm-penetrating ability.

Cytotoxicity assay showed that LipoSC had no obvious cytotoxicity to human gastric carcinoma AGS cells. Additionally, LipoSC-MELB4 did not show significant cytotoxicity at concentrations below 100 μg/mL (Figure 3c), which was lower than the concentration for linolenic acid liposomes.[29] The cytotoxicity of LipoSC-MELB4 occurred at the concentration over 100 μg/mL which may be caused by the incorporation of the MEL-B surfactant into the liposome and which disturbs the stability of the AGS cell membrane at a high concentration. However, this evaluation was performed only under in vitro conditions. Further in vivo evaluation of toxicity showed that oral gavage administration of LipoSC-MELB4 at a high dose (2 g/kg) did not induce significant weight loss or negative effects in mice during a 7 day period (Figure 3d), indicating that LipoSC-MELB4 is biologically safe when administered orally.

Gastric Retention and Mucus and Biofilm Penetration of SC-MELB Liposomes. Besides acid stability, the retention and distribution of amoxicillin-loaded SC-MELB liposomes in the stomach are other important indications for effective gastromucosal drug delivery. Therefore, we examined the retention of LipoSC-MELB4 labeled with Alexa Fluor 594 cadaverine dye (FL594; LipoSC-MELB4/AMX-FL594). LipoSC-MELB4/AMX-FL594 was intragastrically administered to healthy mice. In vivo imaging indicated strong fluorescence in the stomach of the mice 0.5 h after administration (Figure 4b), and it was retained up to 4 h after administration (Figure 4c). In contrast, no detectable fluorescence was observed in the control group treated with PBS (Figure 4a). Ex vivo imaging showed strong fluorescence in the mice stomach tissues at 0.5 and 4 h after treatment, whereas only very weak fluorescence was observed in the stomach of mice in the control group (insets in Figure 4a−c). These observations indicated that LipoSC-MELB4/AMX could be retained in the stomach for at least 4 h.

Next, transverse cryosections of the stomachs from the treated and untreated mice (4 h after treatment) were examined to determine the distribution of LipoSC-MELB4/AMX. Generally, bright fluorescence of FL594 was localized in the mucus layer on the luminal side of the stomach of the mice (Figure 4d−f)[29] but not in the negative control group-administered PBS (Figure S2). These results indicated that LipoSC-MELB4/AMX permeated into the mucus layer of the stomach.

Moreover, in vitro assay using LipoSC-MELB4 coencapsulating AMX and fluorescein sodium confirmed that LipoSC-MELB4/AMX could penetrate freshly prepared porcine mucus within 4 h (Figure 4g−l), with a Papp value of 11.1×10^{-7} cm/s and an aggregation rate of 27.3% (Figure S3). These results were consistent with previous findings on PEGylated lipid polymer nanoparticles of mixed lipid (containing rhamnolipid)-coated chitosan with a negative surface charge.[30] Additionally, the findings of the present study provide evidence that nanoparticles with a negatively charged surface can penetrate the mucus layer of the stomach more easily than those with a positively charged surface, which would form aggregates with negatively charged mucin as a result of electrostatic interactions.[30] In contrast, LipoSC/AMX with a larger particle size of 128.4 nm and lower density of a negative charge of −29.5 mV had a Papp value and liposome-mucus aggregation rate of only 4.1×10^{-7} cm/s and 37% (Figure S3), respectively. Therefore, it was concluded that the relatively small size (∼100 nm) and high density of anionic surface charges[26,29] facilitated the mucosal penetration by LipoSC-MELB4/AMX. Overall, these results indicated that LipoSC-MELB4/AMX could overcome the mucus-layer barrier and deliver the loaded amoxicillin to the site of *H. pylori* infection.[29]

Notably, *H. pylori* biofilms serve as another barrier limiting the efficacy of antibiotic treatment.[6] Therefore, the activity of LipoSC-MELB4/AMX against *H. pylori* biofilms was examined using an in vitro assay. Preliminary results showed that LipoSC-MELB4/AMX was effective against *H. pylori* biofilms. Analysis using Nile red-labeled LipoSC-MELB4 and laser confocal microscopy showed that LipoSC-MELB4 penetrated the biofilm within 30 min (Figure 4m−o). This result indicated that LipoSC-MELB4 could pass through the biofilm barrier of *H. pylori* and deliver its encapsulated amoxicillin for an improved treatment outcome. Moreover, LipoSC-MELB4/AMX was more effective than free amoxicillin against *H. pylori* biofilms (Figure 3b).

Several conventional inorganic and novel organic nanoparticles have been developed against bacterial biofilms.[51,52] However, only limited studies have specifically evaluated their efficacy against *H. pylori* biofilms, making the findings of the present study considerably relevant. Based on the retention and diffusion characteristics and in vitro effects of LipoSC-MELB4/AMX, it was speculated that these liposomes could be effective against *H. pylori* in vivo.

In Vivo Anti-*H. pylori* Efficacy of Amoxicillin-Loaded SC-MELB Liposomes. To evaluate the in vivo therapeutic efficacy of LipoSC-MELB4/AMX against *H. pylori*, mice were infected with *H. pylori*. Before that, gastric ulcers were induced in mice, as *H. pylori* infection is always associated with peptic ulcer disease.[35] Thereafter, the ulcer-harboring mice were administered *H. pylori* SS1 strain via oral gavage, while another group of mice were administered 1 × PBS as the negative control. After 14 days, inoculation was aborted, mice were sacrificed, and the stomachs of the mice were excised to confirm *H. pylori* infection. Anatomical observations (Figure S4a), urease activity determination (Figure S4b), bacterial burden determination ($4.8 \pm 1.8 \times 10^5$ CFU/g), and histopathologic and microscopy examination (Figure S4c−f) confirmed successful *H. pylori* colonization in the gastric mucus.[53] The assembly of *H. pylori* cells observed after performing Giemsa staining suggested the formation of the biofilm.

Next, *H. pylori*-infected mice were divided into three treatment groups: LipoSC-MELB4/AMX (dosage weighed in

https://doi.org/10.1021/acsomega.2c02953
ACS Omega 2022, 7, 29086−29099

(a)

	LipoSC-MELB4/AMX	AMX	PBS
H. pylori burden (CFU/g tissues)	$4.2 \times 10^2 \pm 1.3 \times 10^2$	$5.3 \times 10^3 \pm 1.5 \times 10^3$	$4.6 \times 10^5 \pm 2.2 \times 10^5$

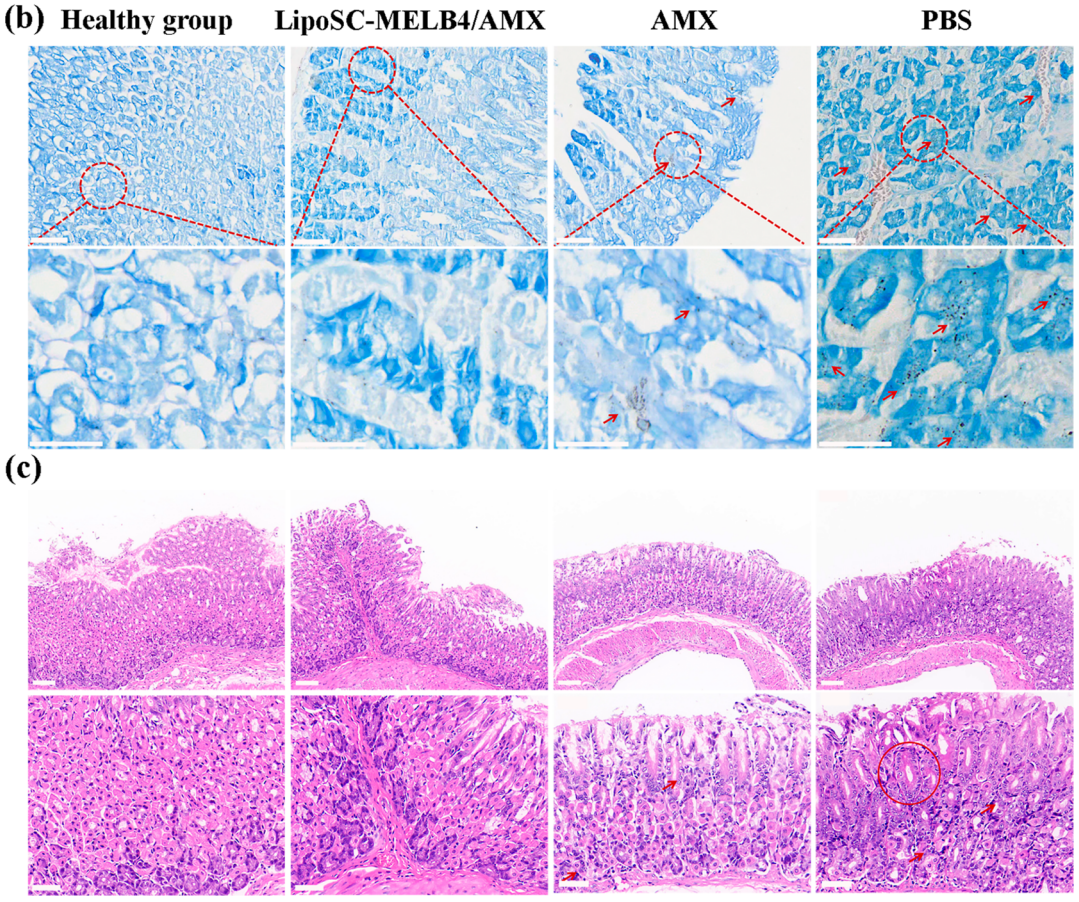

Figure 5. Evaluation of in vivo therapeutic efficacy in *H. pylori*-infected mouse. (a) Bacterial burden in the stomach tissues after different treatments. (b) Upper panel: images of Giemsa-stained stomach tissues, indicating the presence of *H. pylori* (red arrows); scale bar: 50 μm. Lower panel: magnified images for areas in the red dotted circles in the upper panel; scale bar: 25 μm. (c) Images of H & E staining of stomach tissues after different treatments, indicating abnormal hyperplasia (red circle) and inflammatory cell infiltration (red arrows); scale bar in the upper panel: 100 μm; scale bar in the lower magnified panel: 50 μm.

amoxicillin at 14 mg/kg),[54] free amoxicillin (14 mg/kg) as the positive control group, and 1 × PBS as the negative control group. Healthy mice were used for a comparison. A proton pump inhibitor was administered to the mice in the free amoxicillin group 30 min before administration to neutralize gastric acid and prevent drug degradation.[29] After 7 day treatment, in vivo therapeutic efficacy was evaluated. The LipoSC-MELB4/AMX-treated group had the lowest *H. pylori* burden (4.2×10^2 CFU/g) at the end of the treatment period (Figure 5a), followed by the AMX-treated group (5.3×10^3 CFU/g) and PBS-treated group (4.6×10^5 CFU/g). Moreover, Giemsa staining indicated considerably lower *H. pylori* burden in the mucosal tissues of LipoSC-MELB4/AMX-treated mice and healthy mice compared with free amoxicillin and PBS-treated groups (Figure 5b). These results indicated that LipoSC-MELB4/AMX was effective against *H. pylori* in vivo.

Histological assessment using H & E staining (Figure 5c) indicated obvious pathological changes in the gastric mucosa of the PBS group compared with the healthy group, which manifested as highly abnormal hyperplasia composed of irregular glands with complex structural changes (red circle), and a large number of inflammatory cell infiltrates (red arrows), similar to findings reported in a previous study.[38] In contrast, gastric mucosal inflammation was slightly reduced after the administration of free amoxicillin. However, gastric mucosa inflammation disappeared after the LipoSC-MELB4/AMX administration, and there was no significant histological difference between LipoSC-MELB4/AMX-treated mice and mice in the healthy group. Previous studies have clarified that the increased expression of pro-inflammatory cytokines, such as TNF-α and IL-1β, was associated with *H. pylori* infection.[55] The findings of the present study showed decreased expression of pro-inflammatory cytokines, including TNF-α and IL-1β, in the LipoSC-MELB4/AMX-treated group and healthy mice

https://doi.org/10.1021/acsomega.2c02953
ACS Omega 2022, 7, 29086−29099

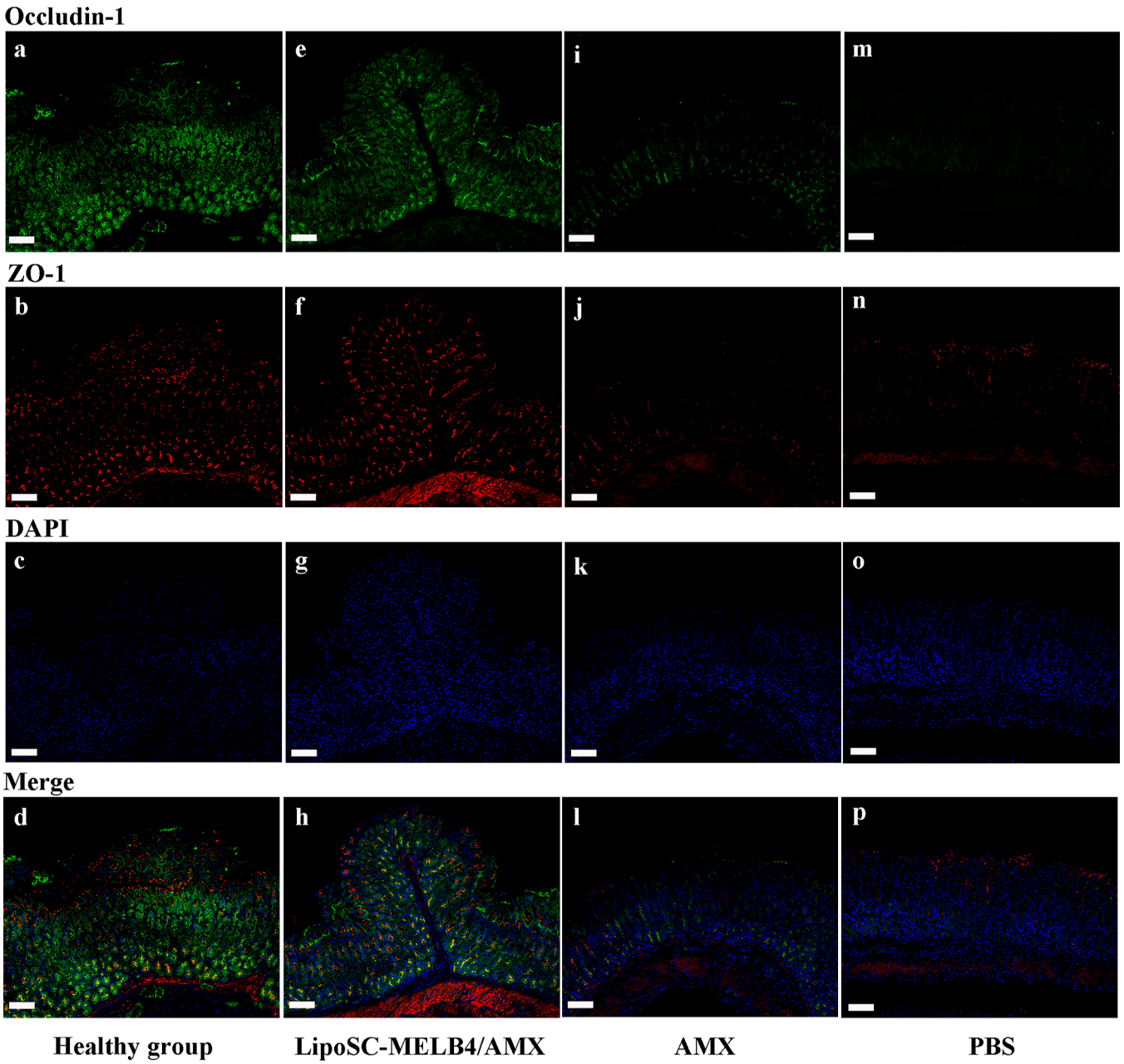

Figure 6. Confocal laser microscopy images for the expression of transmembrane occludin-1 and zonula occludens-1 (ZO-1) proteins involved in gastric mucosal repair in mice, the corresponding DAPI-stained nucleuses, and their merged images of healthy mice (a−d), LipoSC-MELB4/AMX-treated infected mice (e−h), AMX-treated infected mice as the positive control group (i−l), and 1 × PBS-treated infected mice as the negative control group (m−p); scale bar: 100 μm.

compared with the AMX- and PBS-treated groups (Figure S5). These results indicated that LipoSC-MELB4/AMX was effective in ameliorating gastritis-associated inflammations.

Next, the expression of occludin-1 and zonula occludens-1 proteins was investigated in gastric mucosa obtained from peptic ulcers. Tight junction is an important part of the epithelial mucosal barrier, which is composed of multiple proteins, including transmembrane, peripheral membrane, and cytoskeletal proteins.[38] Notably, the transmembrane protein occludin-1 is responsible for regulating the permeability of tight junctions and maintaining cell polarity, whereas zonula occludens-1 (ZO-1) protein plays key roles in gastric mucosal repair.[38] Therefore, in the present study, gastric epithelial cells were stained with immunofluorescence probes to label occludin-1 and ZO-1.[38] In the healthy and LipoSC-MELB4/AMX-treated mice, confocal fluorescence microscopy observation (Figure 6) revealed strong fluorescence on the membrane of the mucosal epithelium and glandular epithelium and in the proximal cytoplasmic region of the cell membranes, indicating the positive expression of these two proteins (Figure 6a−h). In contrast, considerably downregulated expression of occludin-1 and ZO-1 was observed in the AMX- and PBS-groups (Figure 6i−l), with the PBS-treated group showing the weakest expression level (Figure 6m−p). These results indicated that LipoSC-MELB4/AMX was more effective than free amoxicillin in gastric mucosal repair and acted via promoting the expression of mucosa repair proteins.

https://doi.org/10.1021/acsomega.2c02953
ACS Omega 2022, 7, 29086−29099

Overall, our results in this work validate a favorable in vivo treatment efficacy of *H. pylori* infection and its associated symptoms using LipoSC-MELB4/AMX developed in this work. These in vivo therapeutic effects can be attributed to the protection of amoxicillin against the acidic environment of the stomach, as well as the sustained drug release, mucus retention, and mucus and biofilm penetration of LipoSC-MELB4 as revealed by those in vitro or ex vivo evaluations mentioned above, which all would contribute to the enhanced gastromucosal delivery efficacy and improved bioavailability thereof for amoxicillin, as illustrated in Figure 7. This curing efficiency

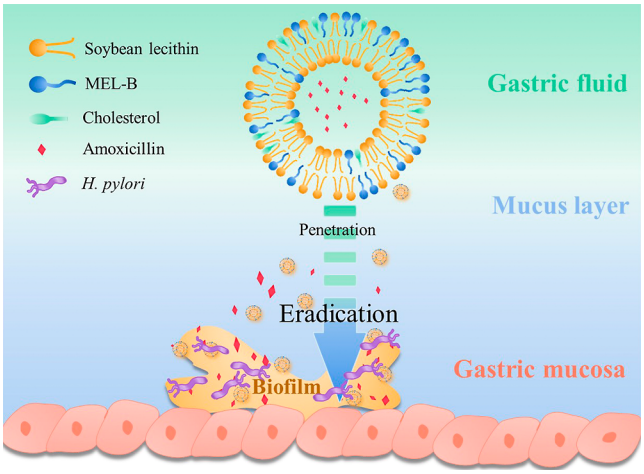

Figure 7. Schematic illustration of the composition and structure of mannosylerythritol lipid-B-incorporated liposomes and its suggested movement through the gastric mucus and biofilm barriers to achieve improved bioavailability and efficient delivery of amoxicillin for the eradication of *H. pylori* infection.

of the liposome here outperforms that of liposomal linolenic acid.[28] Moreover, the easy availability of materials and fabrication of LipoSC-MELB4 highlight its prospect in translation. Thus, the amoxicillin-delivering liposome system developed in the present study possesses several advantages over those reported earlier.[8,11,25]

CONCLUSIONS

In the present study, we showcased that cosmetic raw materials of SL, cholesterol, and mannosylerythritol lipid-B (MEL-B) could also be used to develop a novel efficient gastromucosal delivery system for amoxicillin to treat *H. pylori*. Interestingly, the incorporation of MEL-B induced stronger hydrogen-bond formation and improved the stability of the resulting liposome (LipoSC-MELB) against the extreme acidic environment of the stomach. Additionally, LipoSC-MELB exhibited sustained drug release capacity over a wide pH range, biocompatibility, ability to penetrate the gastric mucus layer, and disrupt *H. pylori* biofilm formation. These features establish LipoSC-MELB as an effective carrier of amoxicillin for improving the latter's bioavailability to achieve enhanced antibacterial activity. Furthermore, the findings of this study showed that amoxicillin-loaded LipoSC-MELB was effective against *H. pylori* both in vitro and in vivo. Moreover, administering amoxicillin-loaded LipoSC-MELB facilitated mucosal repair by downregulating the expression of proinflammatory cytokines and upregulating the expression of mucosal repair proteins. Although our findings propose a potential therapeutic agent against *H. pylori* infection, the efficacy of this drug delivery system could not be confirmed clinically in the present study, which remains its major limitation. Therefore, clinical studies should be performed in the future to examine the efficacy of this drug delivery system for human application.

ASSOCIATED CONTENT

Supporting Information

The Supporting Information is available free of charge at https://pubs.acs.org/doi/10.1021/acsomega.2c02953.

Changes in average particle size and PDI under different pH conditions for liposomes in this work; fluorescence- and bright-field confocal laser microscopy images for the transverse cryosections of mouse stomach tissues administered with 1 × PBS via oral gavage; apparent permeability coefficient and aggregation rate in porcine mucus of LipoSC-MELB4 and LipoSC within 4 h; evaluation of *H. pylori* infection in model mouse; expression levels of proinflammatory cytokines IL-1β and TNF-α in *H. pylori*-infected mice after treatment with PBS, AMX, LipoSC/MELB-AMX, and healthy group; average particle size, PDI, and ζ potential of LipoSC; and EE and DL of different liposome formations (PDF)

AUTHOR INFORMATION

Corresponding Author

Chenguang Liu − *College of Marine Life Sciences, Ocean University of China, Qingdao 266003, China;* orcid.org/0000-0002-9995-4853; Email: liucg@ouc.edu.cn

Authors

Yanping Wu − *College of Marine Life Sciences, Ocean University of China, Qingdao 266003, China*

Jiayue Geng − *College of Marine Life Sciences, Ocean University of China, Qingdao 266003, China*

Xiaohong Cheng − *College of Marine Life Sciences, Ocean University of China, Qingdao 266003, China*

Ying Yang − *College of Marine Life Sciences, Ocean University of China, Qingdao 266003, China; Qingdao Youdo Bioengineering Co. Ltd., Qingdao 266101, China*

Yu Yu − *College of Marine Life Sciences, Ocean University of China, Qingdao 266003, China; Qingdao Youdo Bioengineering Co. Ltd., Qingdao 266101, China*

Lili Wang − *Central Laboratory and Department of Gastroenterology, Qingdao Municipal Hospital, Qingdao 266071, China*

Quanjiang Dong − *Central Laboratory and Department of Gastroenterology, Qingdao Municipal Hospital, Qingdao 266071, China*

Zhe Chi − *College of Marine Life Sciences, Ocean University of China, Qingdao 266003, China;* orcid.org/0000-0002-8794-1940

Complete contact information is available at: https://pubs.acs.org/10.1021/acsomega.2c02953

Author Contributions

Y.W. and J.G. contributed equally. Z.C. and C.G.L. designed and conceived the study; Y.P.W. and J.Y.G. performed the experiments and processed the experimental data with assistance from X.H.C.; Y.Y. and Y.Y. handled the availability of cosmetic raw materials in this study. L.L.W. instructed the

https://doi.org/10.1021/acsomega.2c02953
ACS Omega 2022, 7, 29086−29099

animal assays; Z.C. wrote the manuscript with kind suggestions from Q.J.D.

Notes

The authors declare no competing financial interest.

■ ACKNOWLEDGMENTS

The authors are grateful for financial support by the Natural Science Foundation of Shandong Province (grant No ZR2018MC010). The authors show great gratitude to the Board Chairman, Mr. Jun Li, for his faith and grant of financial assistance in our work.

■ REFERENCES

(1) Robinson, K.; Atherton, J. C. The Spectrum of Helicobacter-Mediated Diseases. *Annu. Rev. Pathol.* **2021**, *16*, 123−144.
(2) Cong, Y.; Geng, J.; Wang, H.; Su, J.; Arif, M.; Dong, Q.; Chi, Z.; Liu, C. Ureido-modified carboxymethyl chitosan-graft-stearic acid polymeric nano-micelles as a targeted delivering carrier of clarithromycin for Helicobacter pylori: Preparation and in vitro evaluation. *Int. J. Biol. Macromol.* **2019**, *129*, 686−692.
(3) Lopes, D.; Nunes, C.; Martins, M. C.; Sarmento, B.; Reis, S. Eradication of Helicobacter pylori: Past, present and future. *J. Control. Release* **2014**, *189*, 169−186.
(4) Chey, W. D.; Leontiadis, G. I.; Howden, C. W.; Moss, S. F. ACG Clinical Guideline: Treatment of Helicobacter pylori Infection. *Am. J. Gastroenterol.* **2017**, *112*, 212−239.
(5) Zhang, Q.; Wu, W.; Zhang, J.; Xia, X. Eradication of Helicobacter pylori: the power of nanosized formulations. *Nanomedicine* **2020**, *15*, 527−542.
(6) Hathroubi, S.; Servetas, S. L.; Windham, I.; Merrell, D. S.; Ottemann, K. M. Helicobacter pylori Biofilm Formation and Its Potential Role in Pathogenesis. *Microbiol. Mol. Biol. Rev.* **2018**, *82*, e00001−18.
(7) Tshibangu-Kabamba, E.; Yamaoka, Y. Helicobacter pylori infection and antibiotic resistance - from biology to clinical implications. *Nat. Rev. Gastroenterol. Hepatol.* **2021**, *18*, 613−629.
(8) de Souza, M. P. C.; de Camargo, B. A. F.; Fortunato, L.; Carvalho, G. C.; Marena, G. C.; Meneguin, G. D.; Bauab, A. B.; Chorilli, T. M.; Chorilli, M. Highlighting the use of micro and nanoparticles based-drug delivery systems for the treatment of Helicobacter pylori infections. *Crit. Rev. Microbiol.* **2021**, *47*, 435−460.
(9) Allen, T. M.; Cullis, P. R. Liposomal drug delivery systems: from concept to clinical applications. *Adv. Drug Deliv. Rev.* **2013**, *65*, 36−48.
(10) Liu, W.; Ye, A.; Han, F.; Han, J. Advances and challenges in liposome digestion: Surface interaction, biological fate, and GIT modeling. *Adv. Colloid Interface Sci.* **2019**, *263*, 52−67.
(11) Jain, P.; Jain, S.; Prasad, K. N.; Jain, S. K.; Vyas, S. P. Polyelectrolyte coated multilayered liposomes (nanocapsules) for the treatment of Helicobacter pylori infection. *Mol. Pharm.* **2009**, *6*, 593−603.
(12) Santos, R. S.; Dakwar, G. R.; Zagato, E.; Brans, T.; Figueiredo, C.; Raemdonck, K.; Azevedo, N. F.; De Smedt, S. C.; Braeckmans, K. Intracellular delivery of oligonucleotides in Helicobacter pylori by fusogenic liposomes in the presence of gastric mucus. *Biomaterials* **2017**, *138*, 1−12.
(13) Deng, G.; Wu, Y.; Song, Z.; Li, S.; Du, M.; Deng, J.; Xu, Q.; Deng, L.; Bahlol, H. S.; Han, H. Tea Polyphenol Liposomes Overcome Gastric Mucus to Treat Helicobacter Pylori Infection and Enhance the Intestinal Microenvironment. *ACS Appl. Mater. Interfaces* **2022**, *14*, 13001−13012.
(14) Bardonnet, P. L.; Faivre, V.; Boullanger, P.; Ollivon, M.; Falson, F. Glycosylated liposomes against Helicobacter pylori: behavior in acidic conditions. *Biochem. Biophys. Res. Commun.* **2009**, *383*, 48−53.
(15) Fan, L.; Chen, Q.; Mairiyangu, Y.; Wang, Y.; Liu, X. Stable vesicle self-assembled from phospholipid and mannosylerythritol lipid and its application in encapsulating anthocyanins. *Food Chem.* **2021**, *344*, 128649.
(16) Jezierska, S.; Claus, S.; Van Bogaert, I. Yeast glycolipid biosurfactants. *FEBS Lett.* **2018**, *592*, 1312−1329.
(17) Coelho, A. L. S.; Feuser, P. E.; Carciofi, B. A. M.; de Andrade, C. J.; de Oliveira, D. Mannosylerythritol lipids: antimicrobial and biomedical properties. *Appl. Microbiol. Biotechnol.* **2020**, *104*, 2297−2318.
(18) Ding, W.; Hattori, Y.; Qi, X.; Kitamoto, D.; Maitani, Y. Surface properties of lipoplexes modified with mannosylerythritol lipid-a and tween 80 and their cellular association. *Chem. Pharm. Bull.* **2009**, *57*, 138−143.
(19) Jo, M.; Park, K. M.; Park, J. Y.; Yu, H.; Choi, S. J.; Chang, P. S. Microfluidic assembly of mono-dispersed liposome and its surface modification for enhancing the colloidal stability. *Colloids Surf., A* **2020**, *586*, 8.
(20) Savoldi, A.; Carrara, E.; Graham, D. Y.; Conti, M.; Tacconelli, E. Prevalence of Antibiotic Resistance in Helicobacter pylori: A Systematic Review and Meta-analysis in World Health Organization Regions. *Gastroenterology* **2018**, *155*, 1372−1382.
(21) Liu, Y.; Yang, T.; Wei, S.; Zhou, C.; Lan, Y.; Cao, A.; Yang, J.; Wang, W. Mucus adhesion- and penetration-enhanced liposomes for paclitaxel oral delivery. *Int. J. Pharm.* **2018**, *537*, 245−256.
(22) Menikarachchi, M.; Katuwavila, K.; Ekanayake, E.; Thevanesam, V.; Karunaratne, V.; Karunaratne, D. N. Release behaviour of amoxicillin from chitosan coated liposomes derived from eggs. *J. Natl. Sci. Found.* **2016**, *44*, 167−173.
(23) Lopes-de-Campos, D.; M. Pinto, R. M.; Costa Lima, S. A. C.; Santos, T.; Sarmento, B.; Nunes, C.; Reis, S. Delivering amoxicillin at the infection site - a rational design through lipid nanoparticles. *Int. J. Nanomed.* **2019**, *14*, 2781−2795.
(24) Brodkorb, A.; Egger, L.; Alminger, M.; Alvito, P.; Assunção, R.; Ballance, S.; Bohn, T.; Bourlieu-Lacanal, C.; Boutrou, R.; Carrière, F.; Clemente, A.; Corredig, M.; Dupont, D.; Dufour, C.; Edwards, C.; Golding, M.; Karakaya, S.; Kirkhus, B.; Le Feunteun, S.; Lesmes, U.; Macierzanka, A.; Mackie, A. R.; Martins, C.; Marze, S.; McClements, D. J.; Ménard, O.; Minekus, M.; Portmann, R.; Santos, C. N.; Souchon, I.; Singh, R. P.; Vegarud, G. E.; Wickham, M. S. J.; Weitschies, W.; Recio, I. INFOGEST static in vitro simulation of gastrointestinal food digestion. *Nat. Protoc.* **2019**, *14*, 991−1014.
(25) Gottesmann, M.; Goycoolea, F. M.; Steinbacher, T.; Menogni, T.; Hensel, A. Smart drug delivery against Helicobacter pylori: pectin-coated, mucoadhesive liposomes with antiadhesive activity and antibiotic cargo. *Appl. Microbiol. Biotechnol.* **2020**, *104*, 5943−5957.
(26) Lai, S. K.; Wang, Y. Y.; Hanes, J. Mucus-penetrating nanoparticles for drug and gene delivery to mucosal tissues. *Adv. Drug Deliv. Rev.* **2009**, *61*, 158−171.
(27) Chen, X.; Li, P.; Shen, Y.; Zou, Y.; Yuan, G.; Hu, H. Rhamnolipid-involved antibiotics combinations improve the eradication of Helicobacter pylori biofilm in vitro: A comparison with conventional triple therapy. *Microb. Pathog.* **2019**, *131*, 112−119.
(28) Stark, R. M.; Gerwig, G. J.; Pitman, R. S.; Potts, L. F.; Williams, N. A.; Greenman, J.; Weinzweig, I. P.; Hirst, T. R.; Millar, M. R. Biofilm formation by Helicobacter pylori. *Lett. Appl. Microbiol.* **1999**, *28*, 121−126.
(29) Thamphiwatana, S.; Gao, W.; Obonyo, M.; Zhang, L. In vivo treatment of Helicobacter pylori infection with liposomal linolenic acid reduces colonization and ameliorates inflammation. *Proc. Natl. Acad. Sci. U.S.A.* **2014**, *111*, 17600−17605.
(30) Li, P.; Chen, X.; Shen, Y.; Li, H.; Zou, Y.; Yuan, G.; Hu, P.; Hu, H. Mucus penetration enhanced lipid polymer nanoparticles improve the eradication rate of Helicobacter pylori biofilm. *J. Control. Release* **2019**, *300*, 52−63.
(31) Fan, W.; Xia, D.; Zhu, Q.; Li, X.; He, S.; Zhu, C.; Guo, S.; Hovgaard, L.; Yang, M.; Gan, Y. Functional nanoparticles exploit the bile acid pathway to overcome multiple barriers of the intestinal epithelium for oral insulin delivery. *Biomaterials* **2018**, *151*, 13−23.
(32) Liu, C. H.; Cao, J. J.; Zhao, Y.; Zheng, C. X.; Zheng, Y. D.; Liu, Q.; Zhang, Z. Z.; Liu, Y. Low-adhesive, Positively Charged

https://doi.org/10.1021/acsomega.2c02953
ACS Omega 2022, 7, 29086−29099

Nanocapsule for the Treatment of Drug-resistant Bacterial Biofilm Infection. *Acta Polym. Sin.* **2019**, *50*, 300−310.
(33) Chinedu, E.; Arome, D.; Ameh, F. S. A new method for determining acute toxicity in animal models. *Toxicol. Int.* **2013**, *20*, 224−226.
(34) Ahani, E.; Montazer, M.; Toliyat, T.; Mahmoudi Rad, M.; Harifi, T. Preparation of nano cationic liposome as carrier membrane for polyhexamethylene biguanide chloride through various methods utilizing higher antibacterial activities with low cell toxicity. *J. Microencapsul.* **2017**, *34*, 121−131.
(35) Ping, Y.; Hu, X.; Yao, Q.; Hu, Q.; Amini, S.; Miserez, A.; Tang, G. Engineering bioinspired bacteria-adhesive clay nanoparticles with a membrane-disruptive property for the treatment of Helicobacter pylori infection. *Nanoscale* **2016**, *8*, 16486−16498.
(36) Zhang, S.; Lee, D. S.; Morrissey, R.; Aponte-Pieras, J. R.; Rogers, A. B.; Moss, S. F. Early or late antibiotic intervention prevents Helicobacter pylori-induced gastric cancer in a mouse model. *Cancer Lett.* **2014**, *355*, 106−112.
(37) Yu, H. J. Probiotic BIFICO cocktail ameliorates Helicobacter pylori induced gastritis. *World J. Gastroenterol.* **2015**, *21*, 6561−6571.
(38) Zhang, W.; Zhou, Y.; Fan, Y.; Cao, R.; Xu, Y.; Weng, Z.; Ye, J.; He, C.; Zhu, Y.; Wang, X. Metal-Organic-Framework-Based Hydrogen-Release Platform for Multieffective Helicobacter Pylori Targeting Therapy and Intestinal Flora Protective Capabilities. *Adv. Mater.* **2022**, *34*, 2105738.
(39) Bombardelli, E.; Patri, G. F. Complex compounds of bioflavonoids with phospholipids, their preparation and use, and pharmaceutical and cosmetic compositions containing them. European Patent. EP 0275005 B1, 1991.
(40) Tai, K.; He, X.; Yuan, X.; Meng, K.; Gao, Y.; Yuan, F. A comparison of physicochemical and functional properties of icaritin-loaded liposomes based on different surfactants. *Colloids Surf., A* **2017**, *518*, 218−231.
(41) Xiao-juan, Z.; Wei-wan, Z.; Jing, Y.; Hao, S. H. I.; He-jing, L. Preparation and Identification of Octenylsuccinate Sucrose Ester and Its Application in Microencapsulation of Soybean Oil. *Food Sci.* **2009**, *30*, 146−148.
(42) Kura, A. U.; Hussein-Al-Ali, S. H.; Hussein, M. Z.; Fakurazi, S. Preparation of Tween 80-Zn/Al-levodopa-layered double hydroxides nanocomposite for drug delivery system. *Sci. World J.* **2014**, *2014*, 104246.
(43) Lee, M. K. Liposomes for Enhanced Bioavailability of Water-Insoluble Drugs: In Vivo Evidence and Recent Approaches. *Pharmaceutics* **2020**, *12*, 264.
(44) Li, W. J.; Nicol, F.; Szoka, F. C. GALA: a designed synthetic pH-responsive amphipathic peptide with applications in drug and gene delivery. *Adv. Drug Deliv. Rev.* **2004**, *56*, 967−985.
(45) Johansson, M. E.; Sjövall, H.; Hansson, G. C. The gastrointestinal mucus system in health and disease. *Nat. Rev. Gastroenterol. Hepatol.* **2013**, *10*, 352−361.
(46) Schreiber, S.; Konradt, M.; Groll, C.; Scheid, P.; Hanauer, G.; Werling, H. O.; Josenhans, C.; Suerbaum, S. The spatial orientation of Helicobacter pylori in the gastric mucus. *Proc. Natl. Acad. Sci. U.S.A.* **2004**, *101*, 5024−5029.
(47) Zhu, Y.-m.; Gao, L.-j.; Zhao, X.-f.; Lu, J. Quantitative Analysis of Refined Pitches by Curve-Fitting of Fourier Transform Infrared Spectroscopy Spectrum. *Spectrosc. Spectr. Anal.* **2019**, *39*, 765−771.
(48) Yu, H.-Y.; Yao, J.-M. Reinforcing properties of bacterial polyester with different cellulose nanocrystals via modulating hydrogen bonds. *Compos. Sci. Technol.* **2016**, *136*, 53−60.
(49) Yu, H. Y.; Zhang, H.; Song, M. L.; Zhou, Y.; Yao, J.; Ni, Q. Q. From Cellulose Nanospheres, Nanorods to Nanofibers: Various Aspect Ratio Induced Nucleation/Reinforcing Effects on Polylactic Acid for Robust-Barrier Food Packaging. *ACS Appl. Mater. Interfaces* **2017**, *9*, 43920−43938.
(50) Seabra, C. L.; Nunes, C.; Brás, M.; Gomez-Lazaro, M.; Reis, C. A.; Gonçalves, I. C.; Reis, S.; Martins, M. C. L. Lipid nanoparticles to counteract gastric infection without affecting gut microbiota. *Eur. J. Pharm. Biopharm.* **2018**, *127*, 378−386.
(51) Li, X.; Chen, D.; Xie, S. Current progress and prospects of organic nanoparticles against bacterial biofilm. *Adv. Colloid Interface Sci.* **2021**, *294*, 102475.
(52) Liu, Y.; Shi, L.; Su, L.; van der Mei, H. C.; Jutte, P. C.; Ren, Y.; Busscher, H. J. Nanotechnology-based antimicrobials and delivery systems for biofilm-infection control. *Chem. Soc. Rev.* **2019**, *48*, 428−446.
(53) Attaran, B.; Falsafi, T.; Moghaddam, A. N. Study of biofilm formation in C57Bl/6J mice by clinical isolates of Helicobacter pylori. *Saudi J. Gastroenterol.* **2016**, *22*, 161−168.
(54) Kim, S. E.; Memon, A.; Kim, B. Y.; Jeon, H.; Lee, W. K.; Kang, S. C. Gastroprotective effect of phytoncide extract from Pinus koraiensis pinecone in Helicobacter pylori infection. *Sci. Rep.* **2020**, *10*, 9547.
(55) Obonyo, M.; Sabet, M.; Cole, S. P.; Ebmeyer, J.; Uematsu, S.; Akira, S.; Guiney, D. G. Deficiencies of myeloid differentiation factor 88, Toll-like receptor 2 (TLR2), or TLR4 produce specific defects in macrophage cytokine secretion induced by Helicobacter pylori. *Infect. Immun.* **2007**, *75*, 2408−2414.

https://doi.org/10.1021/acsomega.2c02953
ACS Omega 2022, 7, 29086−29099